Proceedings of the ASME 2023 Conference on Smart Materials, Adaptive Structures and Intelligent Systems
SMASIS2023
September 11-12, 2023, Austin. Texas

SMASIS2023- 110811

DEVELOPMENT OF A LASER VIBROMETER-BASED SHEAR WAVE SENSING SYSTEM FOR CHARACTERIZING MECHANICAL PROPERTIES OF VISCOELASTIC MATERIALS

Bowen Cai
Mississippi State University
Mississippi State, MS

Liang Shen
Virginia Tech
Blacksburg, VA

Zhe Pei
Virginia Tech
Blacksburg, VA

Teng Li
Virginia Tech
Blacksburg, VA

Jiali Li
Virginia Tech
Blacksburg, VA

Luyu Bo
Virginia Tech
Blacksburg, VA

Yingshan Du
Virginia Tech
Blacksburg, VA

Zhenhua Tian
Virginia Tech
Blacksburg, VA

ABSTRACT

Characterizing the mechanical properties of viscoelastic materials is critical in biomedical applications such as detecting breast cancer, skin diseases, myocardial diseases, and hepatic fibrosis. Current methods lack the consideration of dispersion curves that depend on material properties and shear wave frequency. This paper presents a novel method that combines noncontact shear wave sensing and dispersion analysis to characterize the mechanical properties of viscoelastic materials. Our shear wave sensing system uses a piezoelectric stack (PZT stack) to generate shear waves and a laser Doppler vibrometer (LDV) integrated with a 3D robotic stage to acquire time-space wavefields. Next, an inverse method is employed for the wavefield analysis. This method leverages multidimensional Fourier transform and frequency-wavenumber dispersion curve regression. Through proof-of-concept experiments, our sensing system successfully generated shear waves and acquired its time-space wavefield in a customized viscoelastic phantom. After dispersion curve analysis, we successfully characterized two material properties (shear elasticity and shear viscosity) and measured shear wave velocities at different frequencies.

Keywords: Laser Doppler vibrometer, Piezoelectric stack, Material property measurement, Dispersion curve analysis, Shear wave elastography

1. INTRODUCTION

Biological soft tissues generally have viscoelastic behavior. In recent decades, methods have been continuously developed to characterize the mechanical properties of viscoelastic materials [1]. Among them, ultrasound shear wave elastography is broadly used for the pathological analysis of viscoelastic soft tissues due to its non-invasive and quantitative characteristics. One of the most common methods is the shear wave dispersion curve analysis[2, 3, 4]. The reason is that the velocities of shear waves in viscoelastic materials are highly dependent on frequencies[5]. Shear wave generation and sensing are critical for the shear wave dispersion analysis. In previous studies, different shear wave generation and sensing methods were used. The most common method for generating shear waves in viscoelastic materials is using acoustic radiation force (ARF) generated by phased-array transducer probes [6, 7]. However, phased-array transducer probes are large and require a large contact area on the sample, in order to acquire strong signals. This limits their applications in small samples[8, 9]. In addition, electromechanical shakers or magnetic coils are also common shear wave generation devices[10, 11]. However, similar to ARF, they are large. In addition, they generate unstable displacement amplitudes, which may cause damage to fragile soft tissues. Therefore, it is necessary to develop a new shear wave sensing system that can generate accurate displacements for small, fragile samples.

This study develops a new piezo stack-LDV shear wave sensing system together with a set of wavefield analysis methods to characterize the mechanical properties of viscoelastic materials. Compared with other methods of shear wave excitation, the piezo stack has smaller dimensions, more accurate displacement outputs, and negligible thermal effect on the sample. Our sensing system generates shear waves and collects time-space wavefields on viscoelastic testing phantoms. Unlike a phased array transducer probe, the LDV can acquire the time-space wavefield with features including contact-free and higher spatial sampling resolution[12]. The wavefield analysis methods can obtain the material's mechanical properties from the measured time-space wavefield.

In this paper, Section 2 briefly describes the shear wave generation and acquisition system. Section 3 presents the wavefield processing methods, and Section 4 presents a proof-of-concept experimental study for characterizing the mechanical properties of viscoelastic materials.

2. MECHANISM AND DESIGN OF A PIEZO STACK – LDV SHEAR WAVE SENSING SYSTEM

The piezo stack-LDV shear wave sensing system (Fig. 1a) is composed of a shear wave generating module and a wavefield acquisition module. For the shear wave generation, the top end of a piezo stack is installed on a customized 3D-printed fixture, a 3D-printed hemisphere tip is attached on the bottom end, and the piezo stack is pushed against the test sample (*e.g.*, a viscoelastic phantom). For the shear wave acquisition, a noncontact laser Doppler vibrometer (LDV) with a laser beam normal to the top surface of the viscoelastic phantom is used to acquire the out-of-plane velocities/displacements of shear waves propagating the sample based on the Doppler effect.

In our sensing system, the two modules work together and are controlled by customized codes. To generate shear waves, an excitation signal generated by a function generator and further amplified by a voltage amplifier is sent to the piezo stack to generate shear waves in the phantom. We perform a point-by-point measurement along a user-defined scanning line to obtain the waveform at each scanning point by using the LDV (Fig. 1b). Then, the acquired signals are fused to obtain the 1D wavefield *u(t, x)*, which is a function of the acquired shear wave amplitude versus time *t* and position *x* (Fig. 1c).

In order to correctly obtain the frequency and wavenumber information of the shear wave, the Shannon sampling theorem should be followed. For the sampling in time, the theorem also works, *i.e.*, the sampling frequency should be at least twice the maximum wave frequency being used. Similarly, the spatial sampling resolution should be smaller than a half wavelength.

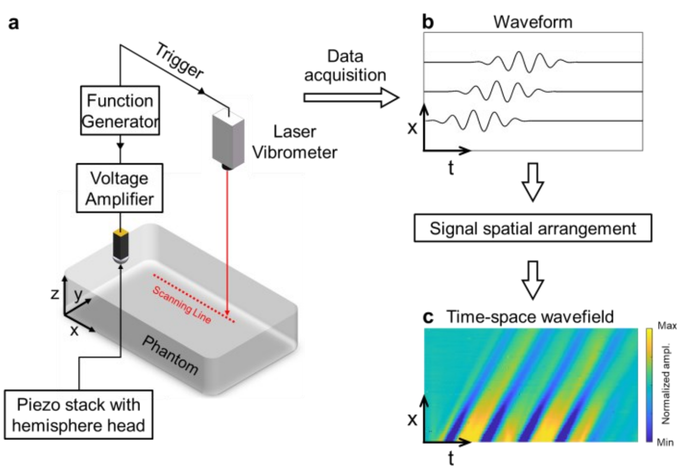

FIGURE 1: ILLUSTRATION OF The PIEZO STACK – LDV SHEAR WAVE SENSING SYSTEM

3. TIME-SPACE WAVEFIELD PROCESSING

To characterize a material's viscoelastic properties, we can measure the velocities or wavenumbers of shear waves at different frequencies and then analyze the dispersion relation. The wavefield measured by our system contains the dispersion information of shear waves in viscoelastic materials, and this information needs to be extracted through wavefield analysis. Here, a dispersion curve regression-assisted wavenumber analysis method is presented. Fig. 2 shows a diagram of this analysis method. The time-space wavefield acquired through our piezo stack-LDV sensing system is firstly processed by the multi-dimensional Fourier transform to obtain a frequency-wavenumber spectrum (Fig. 2a). This spectrum contains the frequency-wavenumber relation of shear waves propagating along the scanning line. This spectrum is compared to a series of theoretical dispersion curves derived from the Kelvin-Voigt model. Then, the theoretical curve that best matches the experimental spectrum is found through a regression process (Fig. 2b), and the material properties for deriving that dispersion curve are recorded. These material properties are considered to be the properties measured by our approach that fuses the piezo stack-LDV shear wave sensing system and the aforementioned wavefield analysis method.

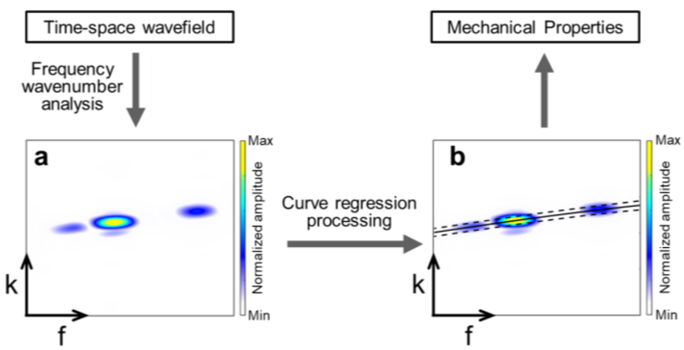

FIGURE 2: DIAGRAM OF THE DISPERSION CURVE REGRESSION-ASSISTED WAVENUMBER ANALYSIS METHOD.

3.1 Frequency-wavenumber processing

The space-time wavefield u $(t,$ $\boldsymbol{x})$ (shown in Fig. 1c) obtained by the LDV is a function of the time variable t and the position $\boldsymbol{x}$. In order to obtain the wave number information from the space-time wavefield, it is necessary to perform a multidimensional Fourier transform on u $(t,$ $\boldsymbol{x})$ to obtain the frequency-wave number representation $U\,(f, \boldsymbol{k})$[13]:

$$U(f,\boldsymbol{k}) = \int_{-\infty}^{\infty}\int_{-\infty}^{\infty} u(t,\boldsymbol{x})e^{-j(2\pi ft-\boldsymbol{k}\cdot\boldsymbol{x})}dtd\boldsymbol{x}, \qquad (1)$$

where the $\boldsymbol{x}$ is the space vector and $\boldsymbol{k}$ is the wavenumber vector.

In this paper, we used the LDV to scan the wavefield along a straight line. Therefore, the space vector $\boldsymbol{x}$ should be reduced to x. The wavefield $u(t, \boldsymbol{x})$ should be reduced to $u(t, x)$, and the two-dimensional Fourier transform should be used [14]:

$$U(f, k_x) = \int_{-\infty}^{\infty}\int_{-\infty}^{\infty} u(t,x)e^{-j(2\pi f t - k_x x)}dtdx. \qquad (2)$$

3.2 Dispersion curve regression for mechanical property characterization

In viscoelastic materials, the frequency-wavenumber dispersion relation of shear waves changes with the mechanical property. This relation can be derived by using the Kelvin-Voigt model [5, 6, 16] and the material properties including elasticity and viscosity coefficient. We assume that the viscoelastic materials in our study fit the Kelvin-Voigt viscoelastic model, which consists of a dashpot (provide shear viscosity μ_1) and a spring (provide shear elasticity μ_2) in parallel. (Fig. 3 top right). For the Kelvin-Voigt model, the stress-strain relation can be expressed as

$$\sigma = \left(\mu_1 - \mu_2 \frac{\partial}{\partial t}\right)\varepsilon, \qquad (3)$$

where σ is shear stress, ε is the shear strain, μ_1 is the shear elasticity, and μ_2 is the shear viscosity. By combining this equation (3) with the strain-displacement relation and the equation of motion, the shear wave equation can be derived,

$$\mu_1 \frac{\partial^2 u_z}{\partial x^2} - \mu_2 \frac{\partial^3 u_z}{\partial x^2 \partial t} = \rho \frac{\partial^2 u_z}{\partial t^2}. \qquad (4)$$

By substituting the wave displacement $u_z = U_z(\omega)e^{i(\omega t - kx)}$ into equation (4), we can derive

$$(-\mu_1 k^2 + i\omega\mu_2 k^2 + \rho\omega^2)U_z(\omega) = 0. \qquad (5)$$

Because $U_z(\omega)$ is a nonzero term, the expression in the parathesis needs to be zero. Thus we can obtain the frequency-wavenumber relation,

$$k = \sqrt{\frac{\rho\omega^2}{\mu_1 + i\omega\mu_2}} = Re\{k\} - iIm\{k\}, \qquad (6)$$

$$Re\{k\} = \sqrt{\frac{\rho\omega^2\left(\sqrt{\mu_1^2 + \omega^2\mu_2^2} + \mu_1\right)}{2(\mu_1^2 + \omega^2\mu_2^2)}}, \qquad (7)$$

$$Im\{k\} = \sqrt{\frac{\rho\omega^2\left(\sqrt{\mu_1^2 + \omega^2\mu_2^2} - \mu_1\right)}{2(\mu_1^2 + \omega^2\mu_2^2)}}. \qquad (8)$$

Re$\{k\}$ and Im$\{k\}$ represent the real and imaginary parts of the wavenumber k, respectively. With the wavenumber, the shear wave velocity C_T and the attenuation α_T can further be derived as

$$C_T = \frac{\omega}{Re\{k\}}, \qquad (9)$$

$$\alpha_T = Im\{k\}, \qquad (10)$$

For viscoelastic materials, the frequency of shear waves generally does not exceed 1000 Hz [6, 18, 19]. Assuming the shear wave frequency ranges from 1 to 1000Hz, a MATLAB code is developed to draw a series of theoretical wavenumber-frequency dispersion curves for different viscoelastic properties (*e.g.*, μ_1 and μ_2), in order to investigate their effects on dispersion curves. As shown in Fig. 3, the wavenumber of the viscoelastic material changes with the frequency f, μ_1, and μ_2. It can be found that μ_1 dominatly affects the low-frequency (*e.g.*, 0-500Hz) wavenumber, while μ_2 dominatly affects the high-frequency (*e.g.*, 500-1000Hz) wavenumber. In other words, the wavenumbers in low and high frequencies are more sensitive to the changes of μ_1 and μ_2, respectively.

With the theoretical shear wave frequency-wavenumber dispersion curves corresponding to different material properties, we can compare these curves to the experimentally acquired frequency-wavenumber spectrum. Through comparison, the theoretical shear wave dispersion curve that best matches the spectrum data can be further found through least square curve regression. The μ_1 and μ_2 values corresponding to the best-fitting theoretical dispersion curve are considered as the measured viscoelastic properties of the test sample.

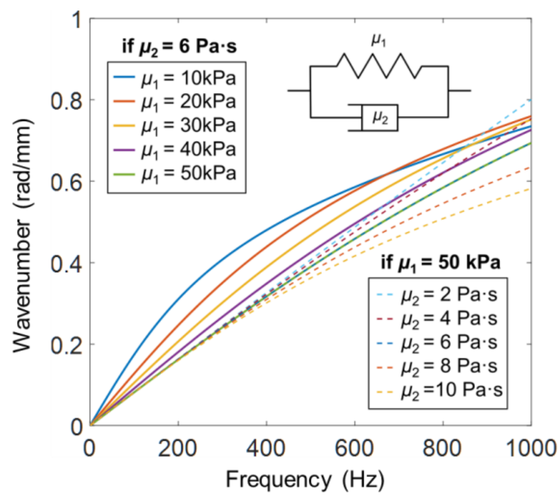

FIGURE 3: THEORETICAL SHEAR WAVE DISPERSION CURVES for VISCOELASTIC MATERIALS WITH DIFFERENT SHEAR ELASTICITY AND SHEAR VISCOSITY

4. EXPERIMENT VALIDATION

To validate our method, we fabricated a viscoelastic phantom using synthetic gelatin. With the fabricated sample, an experiment is performed using the piezo stack-LDV sensing system established in this study. With the acquired experimental data, we performed frequency-wavenumber analysis and dispersion curve regression to characterize the phantom's viscoelastic material properties. The experimental results show that our method can successfully generate shear waves in viscoelastic materials and characterize the phantom's viscoelastic properties (*i.e.*, shear elasticity and shear viscosity).

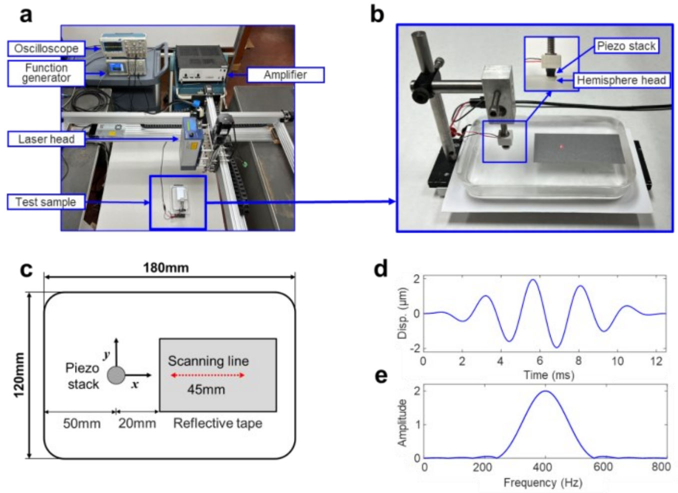

FIGURE 4: EXPERIMENTAL SETUP FOR CHARACTERIZING THE MECHANICAL PROPERTIES OF THE VISCOELASTIC PHANTOM

4.1 Experiments with a viscoelastic phantom

The test sample is a customized phantom (see Fig. 4b) made of synthetic gelatin (Clear Ballistics, USA) with dimensions of $180 \times 120 \times 30$ mm, density of 850 kg/m^3, and longitudinal wave speed of 1560 m/s. A photo of the experimental setup, a zoomed view of the test sample with the piezo stack actuator, and a schematic of the sensing layout with dimensions are given in Fig. 4a, b, and c, respectively. For shear wave generation, a 3D printed hemisphere tip (radius: 5 mm) is attached to the bottom surface of the piezo stack actuator with dimensions of 5×5×10 mm (SMPAK155510D10 by Steminc), and the piezo stack's bottom side is installed on a customized 3D-printed fixture. The piezo stack actuator is pressed on the phantom surface to excite shear waves. The center of the piezo stack actuator is set as the coordinate origin. An arbitrary waveform function generator (Tektronix AFG3052C) is used to generate the excitation signal (a 5-cycle 400 Hz tone burst), which is amplified to 50 Vpp by a voltage amplifier (model: Krohn-Hite 7500). The waveform and frequency spectrum of the excitation are given in Fig. 4d and 4e, respectively. An LDV (model: Polytec OFV-505) is used to measure the out-of-plane displacement components of shear waves and acquire the time-space wavefield along a predefined scanning line with a length of 45mm starting from a point at (40, 0) mm. The spatial sensing resolution is 0.2 mm. The sampling frequency is set to 2.60 kHz.

4.2 LDV Scanning Result and Wavefield-based shear wave velocity determination

The time-space wavefield of shear waves, generated by the piezo stack, is acquired by using the LDV in a point-by-point manner. With the acquired time-space wavefield (Fig. 5), the traditional slope-based method is used to evaluate the shear wave velocity of the phantom. All the wavefield analysis steps in this article are performed using customized codes written in MATLAB (MATLAB 2021a, MathWorks, Inc.).

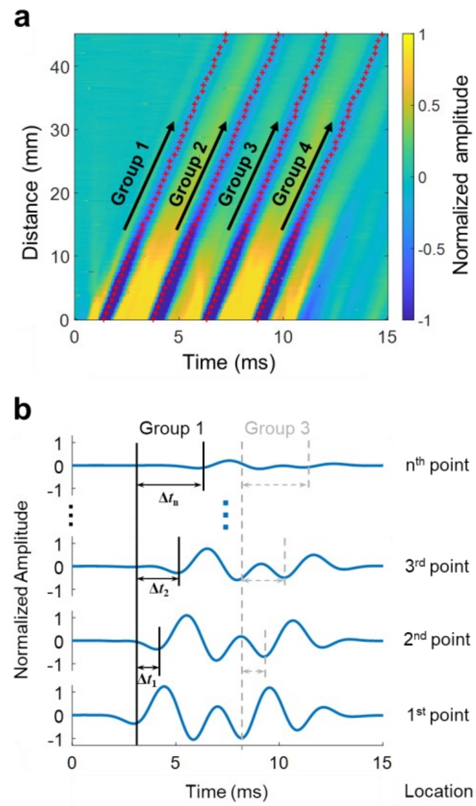

FIGURE 5: ACQUIRED TIME-SPACE WAVEFIELD OF THE SHEAR WAVES AND A SCHEMATIC ILLUSTRATING THE METHOD FOR WAVE VELOCITY DETERMINATION

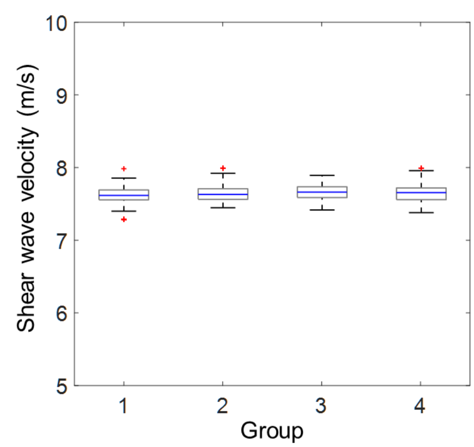

FIGURE 6: MEASURED SHEAR WAVE VELOCITY FOR DIFFERENT MEASUREMENT GROUPS.

Based on the distance from the origin, we sampled and marked the valley positions (with an interval of 1 mm) in the acquired time-space wavefield, as shown in Fig. 5a, and then divided all the sample points into four groups according to the number of valleys. Then, for each group, we calculated the time difference (Δt_n) as illustrated in Fig. 5b. Through the time and the position information, the shear wave velocity can be calculated by the slope formula $C_T = \Delta x_n / \Delta t_n$.

The average velocity of the shear wave in each group is calculated and plotted in Fig. 6. From the statistical result, it can be found that the average velocities of group 1 to 4 are: 7.61 m/s, 7.66 m/s, 7.68 m/s, and 7.67 m/s, respectively. Their average is 7.66 m/s, which is close to the theoretical velocity of 7.71 m/s calculated by equation (9).

4.3 Results by dispersion curve regression

The determination of the shear wave velocity verifies the effectiveness of our piezo stack-LDV shear wave sensing system. The next step is to characterize the material properties of the viscoelastic phantom. Using the method presented in Section 3, both frequency-wavenumber analysis and dispersion curve regression are performed on the acquired wavefield (Fig. 5a). Fig. 7 gives the experimental frequency-wavenumber spectrum, where the highest amplitude points for different frequencies are marked with 'x'. Noticeably, in addition to the shear waves at 400 Hz, the frequency-wavenumber spectrum shows low- and high-frequency components around 200 and 800 Hz respectively. These frequencies match the sub and 2nd harmonic frequencies, which could be induced by the nonlinearity of the piezo stack-based wave generation method. Through the dispersion curve regression processing, the dispersion curve (solid line) that best matches the experimental data is obtained using the method presented in Section 3.2. The dashed lines above and below the solid line in Fig. 7 are the upper and lower boundaries of the 95% confidence interval. The materials properties for the best matching curve are μ_1 of 50kPa and μ_2 of 2.5 Pa·s. Our experimental results, therefore, show that our analysis method is able to characterize the mechanical properties of viscoelastic material.

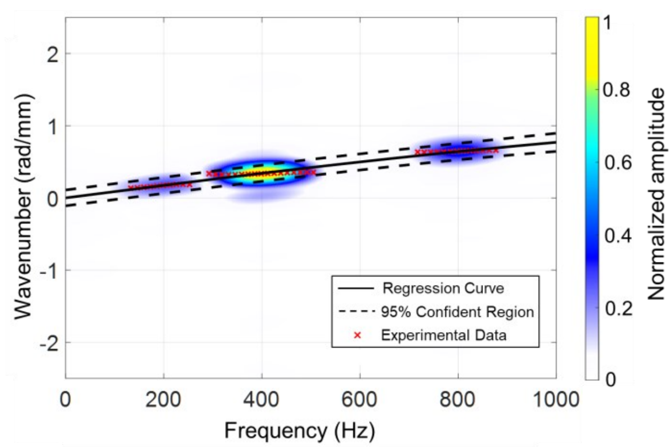

FIGURE 7: EXPERIMENTAL FREQUENCY-WAVENUMBER SPECTRUM OVERLAYED WITH THE DISPERSION CURVE REGRESSION RESULT.

5. CONCLUSION

This paper presents a novel piezo stack – LDV shear wave sensing system, which is able to excite shear waves in viscoelastic materials and measure the time-space wavefields in a contactless and high-resolution manner. To validate our sensing system, we fabricated a viscoelastic synthetic gelatin phantom and designed an experiment. The experimental results show that our method can successfully excite shear waves in the viscoelastic phantom using a piezo stack with a customized ball head and acquire the space-time wavefield of the generated shear waves using the noncontact LDV. By using frequency-wavenumber analysis and dispersion curve regression to process the acquired time-space wavefield, we demonstrated the capability of our method for characterizing the mechanical properties (such as shear elasticity and viscosity) of viscoelastic materials. We expect this research to lead to a noncontact and efficient method for characterizing soft materials, even human tissues, and monitoring their property changes.

ACKNOWLEDGEMENTS

The authors would like to thank the financial supports from Mississippi State University, National Institute of General Medical Sciences of the National Institutes of Health (7R01GM144417), National Science Foundation (CMMI-2243771), and DOE Office of Nuclear Energy's Nuclear Energy University Programs (DE-NE0009187).

REFERENCES

[1] A. Sarvazyan, T. J. Hall, M. W. Urban, M. Fatemi, S. R. Aglyamov, B. S. Garra, An Overview of Elastography-An Emerging Branch of Medical Imaging, Current Medical Imaging Reviews 7 (2011) 255–282.

[2] M. Tanter, J. Bercoff, A. Athanasiou, T. Deffieux, J.L. Gennisson, G. Montaldo, M. Muller, A. Tardivon, M. Fink, Quantitative Assessment of Breast Lesion Viscoelasticity: Initial Clinical Results Using Supersonic Shear Imaging, Ultrasound in Medicine & Biology 34 (2008) 1373–1386.

[3] T. Deffieux, G. Montaldo, M. Tanter, M. Fink, Shear wave spectroscopy for in vivo quantification of human soft tissues visco-elasticity, IEEE Transactions on Medical Imaging 28 (2009) 313–322.

[4] C. Amador, M.W. Urban, S. Chen, J.F. Greenleaf, Shearwave dispersion ultrasound vibrometry (SDUV) on swine kidney, IEEE Transactions on Ultrasonics, Ferroelectrics, and Frequency Control 58 (2011) 2608–2619.

[5] N.C. Rouze, Y. Deng, C.A. Trutna, M.L. Palmeri, K.R. Nightingale, Characterization of Viscoelastic Materials Using Group Shear Wave Speeds, IEEE Transactions on Ultrasonics, Ferroelectrics, and Frequency Control 65 (2018) 780–794.

[6] P. Kijanka, M.W. Urban, Local Phase Velocity Based Imaging (LPVI) of Viscoelastic Phantoms and Tissues, IEEE Transactions on Ultrasonics, Ferroelectrics, and Frequency Control 68 (2021) 389.

[7] J.A. Martin, D.G. Schmitz, A.C. Ehlers, M.S. Allen, D.G. Thelen, Calibration of the shear wave speed-stress relationship in ex vivo tendons, Journal of Biomechanics 90 (2019) 9–15.

[8] T.W.J. Almeida, D.R.T. Sampaio, A.C. Bruno, T.Z. Pavan, A.A.O. Carneiro, Comparison between shear wave dispersion magneto motive ultrasound and transient elastography for measuring tissue-mimicking phantom viscoelasticity, IEEE Transactions on Ultrasonics, Ferroelectrics, and Frequency Control 62 (2015) 2138–2145.
[9] E.G. Simon, S. Callé, F. Perrotin, J.P. Remenieras, Measurement of shear wave speed dispersion in the placenta by transient elastography: A preliminary ex vivo study, PLOS ONE 13 (2018) e0194309.
[10] X. Wang, Y. Geng, D. Han, M. Lu, R. Li, Y. Li, Q. Zhang, M. Wan, Viscoelastic characterization of HIFU ablation with shear wave by using K-space analysis combined with model-fitting correction method, Ultrasonics 108 (2020) 106179.
[11] S. Chen, M. Fatemi, J.F. Greenleaf, Quantifying elasticity and viscosity from measurement of shear wave speed dispersion, Citation: The Journal of the Acoustical Society of America 115 (2004) 2781.
[12] P. Castellini, M. Martarelli, E.P. Tomasini, Laser Doppler Vibrometry: Development of advanced solutions answering to technology's needs, Mechanical Systems and Signal Processing 20 (2006) 1265–1285.
[13] D.H. Johnson, D.E. Dudgeon, Signals in Space and Time, Array Signal Processing: Concepts and Techniques (1992) 533.
[14] Z. Tian, L. Yu, Lamb wave frequency-wavenumber analysis and decomposition, Journal of Intelligent Material Systems and Structures 25 (2014) 1107–1123.
[15] Z. Tian, W. Xiao, Z. Ma, L. Yu, Dispersion curve regression – assisted wideband local wavenumber analysis for characterizing three-dimensional (3D) profile of hidden corrosion damage, Mechanical Systems and Signal Processing 150 (2021) 107347.
[16] S. Catheline, J.-L. Gennisson, G. Delon, M. Fink, R. Sinkus, S. Abouelkaram, J. Culioli, Measurement of viscoelastic properties of homogeneous soft solid using transient elastography: An inverse problem approach, The Journal of the Acoustical Society of America 116 (2004) 3734.
[17] V. Giurgiutiu, Structural health monitoring with piezoelectric wafer active sensors, Elsevier/Academic Press, 2008.
[18] S. Chen, W. Sanchez, M.R. Callstrom, B. Gorman, J.T. Lewis, S.O. Sanderson, J.F. Greenleaf, H. Xie, Y. Shi, M. Pashley, V. Shamdasani, M. Lachman, S. Metz, Assessment of liver viscoelasticity by using shear waves induced by ultrasound radiation force, Radiology 266 (2013) 964–970.
[19] R.J.G. Van Sloun, R.R. Wildeboer, H. Wijkstra, M. Mischi, Viscoelasticity Mapping by Identification of Local Shear Wave Dynamics, IEEE Transactions on Ultrasonics, Ferroelectrics, and Frequency Control 64 (2017) 1666–1673.